

1 **Measurement report: Occurrence of aminiums**  
2 **in PM<sub>2.5</sub> during winter in China: aminium**  
3 **outbreak during polluted episodes and potential**  
4 **constraints**

5

6 Yu Xu<sup>1,2</sup>, Tang Liu<sup>1</sup>, Yi-Jia Ma<sup>1</sup>, Qi-Bin Sun<sup>3</sup>, Hong-Wei Xiao<sup>1,2</sup>, Hao Xiao<sup>1,2</sup>, Hua-  
7 Yun Xiao<sup>1,2\*</sup>, Cong-Qiang Liu<sup>4</sup>

8

9 <sup>1</sup>School of Agriculture and Biology, Shanghai Jiao Tong University, Shanghai 200240,  
10 China

11 <sup>2</sup>Shanghai Yangtze River Delta Eco-Environmental Change and Management  
12 Observation and Research Station, Ministry of Science and Technology, Ministry of  
13 Education, Shanghai 200240, China

14 <sup>3</sup>Dongguan Meteorological Bureau, Dongguan, Guangdong, 523086, China

15 <sup>4</sup>Institute of Surface-Earth System Science, School of Earth System Science, Tianjin  
16 University, Tianjin 300072, China

17

18

19

20

\*Corresponding authors

21

Hua-Yun Xiao

22

E-mail: xiaohuayun@sjtu.edu.cn

23

24

25 **Abstract:** Amines and aminiums play an important role in particle formation, liquid-  
26 phase reactions, and climate change, attracting considerable attention over the years.  
27 Here, we investigated the concentrations and compositions of aminiums in PM<sub>2.5</sub> in  
28 11 Chinese cities during the winter, focusing on the characteristics of aminiums  
29 during the polluted days and the key factors influencing aminium outbreak.  
30 Monomethylaminium was the dominant aminium species in most cities except  
31 Taiyuan and Guangzhou, followed by dimethylaminium. Diethylaminium dominated  
32 the total aminiums in Taiyuan and Guangzhou. Thus, the main amine sources in  
33 Taiyuan and Guangzhou were significantly different from those in other cities. The  
34 concentrations of the total aminiums (TA) in most cities increased significantly during  
35 the polluted days, while relatively weak aminium outbreaks during the polluted days  
36 occurred in Xi'an and Beijing. Additionally, the concentrations of TA in Xi'an and  
37 Beijing were insignificantly correlated with those of PM<sub>2.5</sub> and the major acidic  
38 aerosol components, while the opposite pattern was observed in 9 other cities. Thus,  
39 acid-base chemistry was significantly associated with the formation of aminiums in  
40 PM<sub>2.5</sub> in all cities except Xi'an and Beijing. Based on the sensitivity analysis of the  
41 aminiums/ammonium ratio to ammonium changes as well as excluding the effects of  
42 relative humidity and atmospheric oxidation, we proposed the possibility of the  
43 competitive uptake of ammonia versus amines on acidic aerosols or the displacement  
44 of aminiums by ammonia in Xi'an and Beijing (constraining aminium outbreaks).  
45 Overall, this study deepens the understanding of the spatiotemporal differences in  
46 aminium characteristic and formation in China. However, the uptake of amines on

47 particles to form aminiums and the relevant influencing factors require further  
48 mechanistic research.

49

50 **Keywords:** Aminiums, PM<sub>2.5</sub> pollution, Aerosol acidity, Spatiotemporal variations,  
51 Formation mechanism

52

53

## 54 **1. Introduction**

55 Low-molecular-weight amines are ubiquitous and important in the gaseous and  
56 particulate phases (Nielsen et al., 2012; Ge et al., 2011a; Berta et al., 2023). More  
57 than 150 amines have been identified in the atmosphere (Ge et al., 2011a). The most  
58 abundant and frequently reported amines in field observations are typically C1–C6  
59 alkylamines including dimethylamine, monomethylamine, trimethylamine,  
60 diethylamine, ethylamine, 1-propanamine, and 1-butanamine (Yang et al., 2023b; Liu  
61 et al., 2023). Amines can participate in various chemical and physical processes in the  
62 atmosphere, promoting the formation and growth of new particles and contributing to  
63 the production of secondary organic aerosols (Yao et al., 2018; Tong et al., 2020;  
64 Møller et al., 2020). Amines are thus considered to have a direct or indirect impact on  
65 air quality (Li et al., 2019; Tao et al., 2016; Shen et al., 2023). Air pollution (e.g.,  
66 haze) caused by high levels of atmospheric fine particles (PM<sub>2.5</sub>) has received  
67 considerable attention in China over the past decade due to rapid industrialization and  
68 urbanization (Liu et al., 2022b; Liu et al., 2022c). Evidently, controlling the emission

69 strength of amine sources and understanding the transformation of atmospheric  
70 amines can effectively reduce air pollution in cities.

71 The main sources of atmospheric amines during the air pollution period in cities  
72 in China are typically fossil fuel combustion and biomass burning rather than  
73 agricultural emissions (Feng et al., 2022; Liu et al., 2022c; Wang et al., 2022; Shen et  
74 al., 2017; Ho et al., 2016; Chang et al., 2022). Owing to the water solubility and  
75 alkalinity of amines, low-molecular-weight amines in PM<sub>2.5</sub> during the air pollution  
76 period are mainly present in the form of amine salts (i.e., aminiums) via the gas-to-  
77 particle partitioning of gaseous amines and subsequent acid-base chemistry (Zhang et  
78 al., 2021; Liu et al., 2022a; Ge et al., 2011a; Xie et al., 2018). It should be noted that  
79 organic amines (e.g., dimethylamine and trimethylamine) in nanoparticles (<200 nm)  
80 may also be largely present in the organic phase (Xie et al., 2018). In addition,  
81 oxidative degradation of higher-molecular-weight amines and displacement reactions  
82 are also potential formation pathways of aminiums in PM<sub>2.5</sub> (Tao et al., 2021; Qiu and  
83 Zhang, 2013; Tong et al., 2020). Although previous observational studies have  
84 investigated the compositions, concentrations, sources, and formation processes of  
85 low-molecular-weight aminiums in the particle phase in urban areas of Shanghai (Liu  
86 et al., 2023), Guangzhou (Shu et al., 2023), Qingdao (Liu et al., 2022c), Xuzhou  
87 (Yang et al., 2023b), China, there has been relatively little focus on the association  
88 between PM<sub>2.5</sub> and amine outbreaks. A recent study conducted in Wangdu County,  
89 Hebei Province, China has suggested that amines exhibited outbreak characteristics  
90 during the haze episode (Feng et al., 2022). Climate and air pollution conditions can

91 vary greatly from city to city due to the vastness of China. However, it is poorly  
92 understood how the characteristics and formation processes of low-molecular-weight  
93 aminiums in PM<sub>2.5</sub> vary between clean and polluted days in different cities in China,  
94 which may hinder the further assessment of the environmental impacts of amines with  
95 regional differences.

96 In winter in China, air pollution episodes are more frequent compared to other  
97 seasons. Thus, we present the measurements of aminiums in PM<sub>2.5</sub> collected from 11  
98 different Chinese cities during the winter (2017–2018). The aims of this study are (1)  
99 to investigate the spatial differences in the compositions and concentrations of  
100 aminiums in PM<sub>2.5</sub>, with a focus on the difference between them on clean days and  
101 polluted days, and (2) to understand the key factors controlling the formation of  
102 aminiums in PM<sub>2.5</sub> in different cities.

103

## 104 **2. Materials and Methods**

### 105 **2.1. Site Description and Sample Collection**

106 A total of eleven urban sites were selected for aerosol sample collection,  
107 including Beijing (BJ; 116.41°E, 40.04°N), Taiyuan (TY; 112.58°E, 37.80°N), Xi'an  
108 (XA; 108.98°E, 34.25°N), Lanzhou (LZ; 103.73°E, 36.11°N), Haerbin (HEB, i.e.,  
109 Harbin; 126.64°E, 45.77°N), Wulumuqi (WLMQ, i.e., Urumqi; 87.75°E, 43.86°N),  
110 Chengdu (CD; 104.14°E, 30.68°N), Guiyang (GY; 106.73°E, 26.58°N), Guangzhou  
111 (GZ; 113.35°E, 23.18°N), Wuhan (WH; 114.36°E, 30.55°N), and Hangzhou (HZ;  
112 120.16°E, 30.30°N) sites (**Figure S1**). HZ and GZ are megacities situated in the

113 Yangtze River Delta (YRD) and Pearl River Delta (PRD) regions respectively, both of  
114 which have developed economies. WH is located in the central region of China. CD  
115 and GY are representative cities in southwest China. LZ, XA, TY, BJ, and HEB are  
116 cities in northern China. WLMQ, located in northwest China, is the largest inland city  
117 farthest from the ocean in the world. Obviously, the varying geographical locations  
118 and economic development levels of different cities lead to different air pollution and  
119 climate conditions between them.

120  $PM_{2.5}$  sampling in most cities was conducted on the rooftops of buildings (4–6  
121 floors in total) using a high-volume air sampler (Series 2031, Laoying, China) from  
122 December 1, 2017 to January 21, 2018 (winter). Specifically, the sampling periods in  
123 LZ, TY, HEB, BJ, XA, WLMQ, CD, WH, HZ, GZ, and GY were Dec. 2–30, 2017,  
124 Dec. 2–30, 2017, Dec. 18, 2017 – Jan. 15, 2018, Dec. 22, 2017 – Jan. 21, 2018, Dec.  
125 22, 2017 – Jan. 20, 2018, Mar. 3–28, 2018, Dec. 1 – 31, 2017, Dec. 6–29, 2017, Dec.  
126 4–31, 2017, Dec. 1–30, 2017, and Dec. 10, 2017 – Jan. 11, 2018, respectively (**Tables**  
127 **S1-S3**). At each site,  $PM_{2.5}$  was sampled once every one to two days for ~24 hours on  
128 prebaked quartz fiber filters (500 °C for 8 hours). Moreover, two random blank filters  
129 were collected. The total number of  $PM_{2.5}$  samples at each sampling site was shown in  
130 **Tables S1-S3**. All samples were stored at –30 °C. Meteorological data such as  
131 precipitation, wind speed, temperature, and relative humidity (RH), as well as  
132 concentrations of various pollutants were recorded during the sampling campaigns  
133 from the adjacent environmental monitoring stations. Sampling periods were  
134 classified as either clean or polluted days based on a daily average  $PM_{2.5}$  mass

135 concentration of  $75 \mu\text{g m}^{-3}$  (Zhang and Cao, 2015) .

136

## 137 **2.2. Chemical Analysis**

138 The extraction of low-molecular-weight aminiums in the filter samples was  
139 carried out using the method described in our recent publication (Liu et al., 2023) and  
140 in a previous study (Liu et al., 2017). Briefly, the sample was filtered using a  $0.22 \mu\text{m}$   
141 Teflon syringe filter (CNW Technologies GmbH) after extraction with Milli-Q water  
142 ( $\sim 18.2 \text{ M}\Omega \text{ cm}$ ). The aminiums in the extracts that underwent pH regulation were  
143 derivatized using  $0.1 \text{ mL}$  of benzenesulfonyl chloride (BSC). The tube containing the  
144 derivatives was sealed and agitated for 30 minutes. To remove excess derivatization  
145 reagents, the extracts were agitated again for 30 minutes at  $80^\circ\text{C}$  after adding NaOH  
146 solution ( $0.5 \text{ mL}$  of  $10 \text{ mol L}^{-1}$ ). Once the mixed solution had cooled down, it was  
147 acidified with a solution of HCl to adjust the pH to 5.5. A further extraction of  
148 derivatives was carried out by adding dichloromethane. It is important to mention that  
149 the organic phase was treated with  $\text{Na}_2\text{CO}_3$  solution and anhydrous  $\text{Na}_2\text{SO}_4$   
150 sequentially. A stream of nitrogen gas was used to concentrate the organic extracts.  
151 Finally, the sample was analyzed using GC-MS after adding dichloromethane and  
152 hexamethylbenzene. Dimethylaminium ( $\text{DMAH}^+$ ), monomethylaminium ( $\text{MMAH}^+$ ),  
153 diethylaminium ( $\text{DEAH}^+$ ), ethylaminium ( $\text{EAH}^+$ ), propylaminium ( $\text{PAH}^+$ ),  
154 butylaminium ( $\text{BAH}^+$ ), and pyrrolidinium ( $\text{PYRH}^+$ ) were quantified. Aminium  
155 recoveries varied between 73% for  $\text{DMAH}^+$  and 112% for  $\text{PAH}^+$ . The detection limits  
156 of the aminium measurements ranged from  $0.8 \text{ ng mL}^{-1}$  for  $\text{DEAH}^+$  to  $2.8 \text{ ng mL}^{-1}$  for

157 MMAH<sup>+</sup>. Aminiums are undetectable in the blank. Detailed data quality controls were  
158 described in our recent publication (Liu et al., 2023). It should be noted that we did  
159 not consider the impact of continuous aging of aminiums collected on the filter on the  
160 measurement results. This is mainly due to the following reasons. The PM<sub>2.5</sub> samples  
161 investigated in this study are all acidic (**Tables S1–S3**), promoting the protonation of  
162 amino groups. The protonated amino group is difficult to undergo oxidation by  
163 oxidants (e.g., hydroxyl radicals and ozone) (Nielsen et al., 2012).

164 Another filter cut was extracted with Milli-Q water to measure the  
165 concentrations of inorganic ions (e.g., NO<sub>3</sub><sup>-</sup>, SO<sub>4</sub><sup>2-</sup>, NH<sub>4</sub><sup>+</sup>, K<sup>+</sup>, Na<sup>+</sup>, Ca<sup>2+</sup>, and Mg<sup>2+</sup>) and  
166 organic acids (e.g., acetic acid, formic acid, succinic acid, oxalic acid, glutaric acid,  
167 and methanesulfonic acid) (Xu et al., 2022a; Xu et al., 2023; Liu et al., 2023; Lin et  
168 al., 2023). These inorganic ions were quantified via an ion chromatograph system  
169 (Dionex Aquion, Thermo Scientific, USA).

170

### 171 **2.3. Parameter calculation**

172 The thermodynamic model (ISORROPIA-II) was used for the prediction of the  
173 mass concentration of aerosol liquid water (ALW) and the pH value, which was  
174 detailed in our previous studies (Xu et al., 2022b; Xu et al., 2020; Xu et al., 2023).  
175 The ventilation coefficient (VC) can be used as an indicator to assess the state of  
176 atmospheric dilution of pollutant concentrations (Gani et al., 2019). It is calculated by  
177 multiplying the wind speed by the planetary boundary layer height (PBLH) (Yang et  
178 al., 2023a).



179

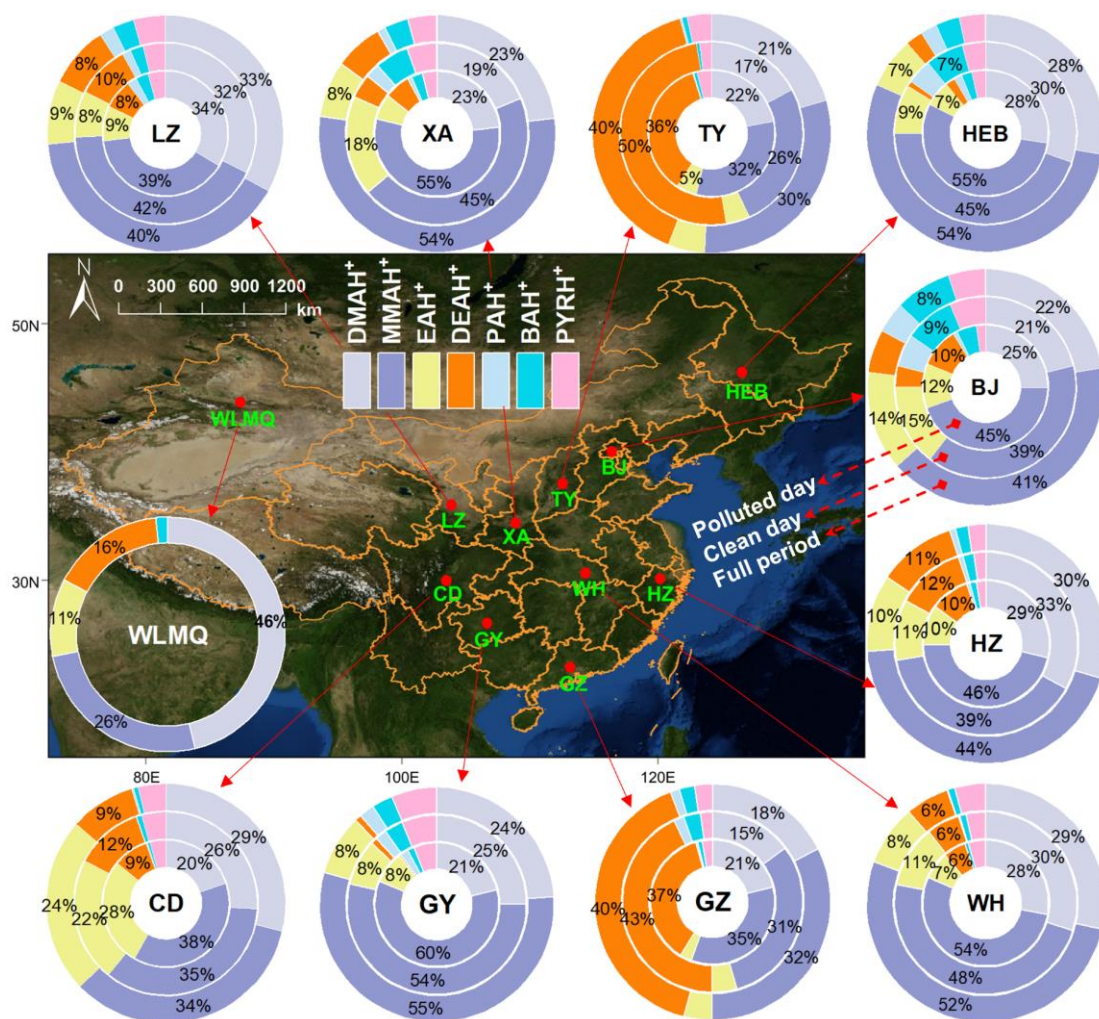
### 180 **3. Results and discussion**

#### 181 **3.1. Compositions of aminiums in PM<sub>2.5</sub> in China during winter**

182 **Figure 1** shows the average percentage distributions of various aminiums in  
183 PM<sub>2.5</sub> collected in different cities in China during winter, with a comparison between  
184 their mass fractions on clean and polluted days. MMAH<sup>+</sup> was the predominant species  
185 among the aminiums investigated in PM<sub>2.5</sub> in most cities in northern China, including  
186 LZ, XA, HEB, BJ, and WLMQ. MMAH<sup>+</sup> and DMAH<sup>+</sup> (as the second most abundant  
187 species) constituted over 63% of the total aminium concentrations in those northern  
188 cities. The relatively minor species, including DEAH<sup>+</sup>, EAH<sup>+</sup>, PAH<sup>+</sup>, BAH<sup>+</sup>, and  
189 PYRH<sup>+</sup>, contributed between 1% and 18% of the total aminium concentrations. The  
190 predominance of MMAH<sup>+</sup> was also found in cities in the YRD (HZ), central (WH),  
191 and southwestern (CD and GY) China, closely followed by DMAH<sup>+</sup>. Previous studies  
192 conducted in Xi'an (winter, China) (Ho et al., 2015), Beijing (winter, China) (Wang et  
193 al., 2022; Ho et al., 2016), Nanjing (winter, China) (Liu et al., 2023) Shanghai (winter,  
194 China) (Liu et al., 2023), Xiamen (winter, China) (Ho et al., 2016), Hong Kong  
195 (winter, China) (Ho et al., 2016), and Arabian Sea (autumn and winter) (Gibb et al.,  
196 1999), as well as at mountain (autumn, Nanling, China) (Liu et al., 2018) and  
197 background (winter, Pudong, China) (Liu et al., 2023) sites have suggested that the  
198 mass concentration fraction of MMAH<sup>+</sup> was highest in the measured aerosol amine  
199 salts. The Henry's constants of MMA ( $3.65 \times 10^1 \text{ mol kg}^{-1} \text{ atm}^{-1}$ ), DMA ( $3.14 \times 10^1$   
200  $\text{mol kg}^{-1} \text{ atm}^{-1}$ ), and EA ( $3.55 \times 10^1 \text{ mol kg}^{-1} \text{ atm}^{-1}$ ) are relatively lower than those of

201 the other amines investigated (e.g.,  $1.32 \times 10^2 \text{ mol kg}^{-1} \text{ atm}^{-1}$  for DEA) (Ge et al.,  
 202 2011b), implying that the potential of MMA, DMA, and EA to be partitioned into  
 203 aqueous particles was weaker compared to DEA. Additionally, the gaseous forms of  
 204 these determined aminiums typically have strong alkalinity (Ge et al., 2011b). The  
 205 aerosol samples in this study were all acidic (**Tables S1–S3**). Thus, these results imply  
 206 that the increased emissions of MMA and DMA may partially explain the higher  
 207 abundance of MMAH<sup>+</sup> and DMAH<sup>+</sup> in PM<sub>2.5</sub> in these investigated cities during winter.

208



210 **Figure 1.** Average percentage distributions of various aminiums in PM<sub>2.5</sub> collected in  
211 different cities in China during winter. The map was obtained from ©MeteoInfoMap  
212 (version 3.3.0) (Chinese Academy of Meteorological Sciences, China).

213

214 In another northern city (i.e., TY), DEAH<sup>+</sup> was the most abundant aminium  
215 species (40% of the total aminium concentrations), followed by MMAH<sup>+</sup> (30%) and  
216 DMAH<sup>+</sup> (21%). The composition characteristic of aminiums in the city of GZ (PRD  
217 area) was similar to that observed in TY (**Figure 1**). Anthropogenic emissions,  
218 including vehicle exhaust and industrial production are considered to be the main  
219 contributors to aerosol DEAH<sup>+</sup> in urban areas (Chen et al., 2022b; Chen et al., 2019;  
220 Yang et al., 2023b; Chang et al., 2022). A recent study has suggested that ethanol  
221 gasoline vehicles can emit a large amount of ethyl-amines, leading to the outbreak of  
222 DEAH<sup>+</sup> during the haze episodes in Hebei Province (North China) (Feng et al., 2022).  
223 Thus, the relative emission strength of anthropogenic DEA in the investigated amines  
224 was probably higher in TY (an inland city with application of ethanol gasoline  
225 vehicles) than in other cities. In addition, previous studies have suggested that aerosol  
226 DEAH<sup>+</sup> can also be largely derived from marine emissions (Facchini et al., 2008;  
227 Dall'osto et al., 2019). Since GZ is a developed coastal city, local aerosol aminiums  
228 may be influenced by large gaseous DEA inputs from both local industrial production  
229 and marine sources.

230 The mass concentration fractions of aminiums on clean and polluted days were  
231 also compared (**Figure 1**). The dominant aminium species (i.e., MMAH<sup>+</sup>, DMAH<sup>+</sup>, or

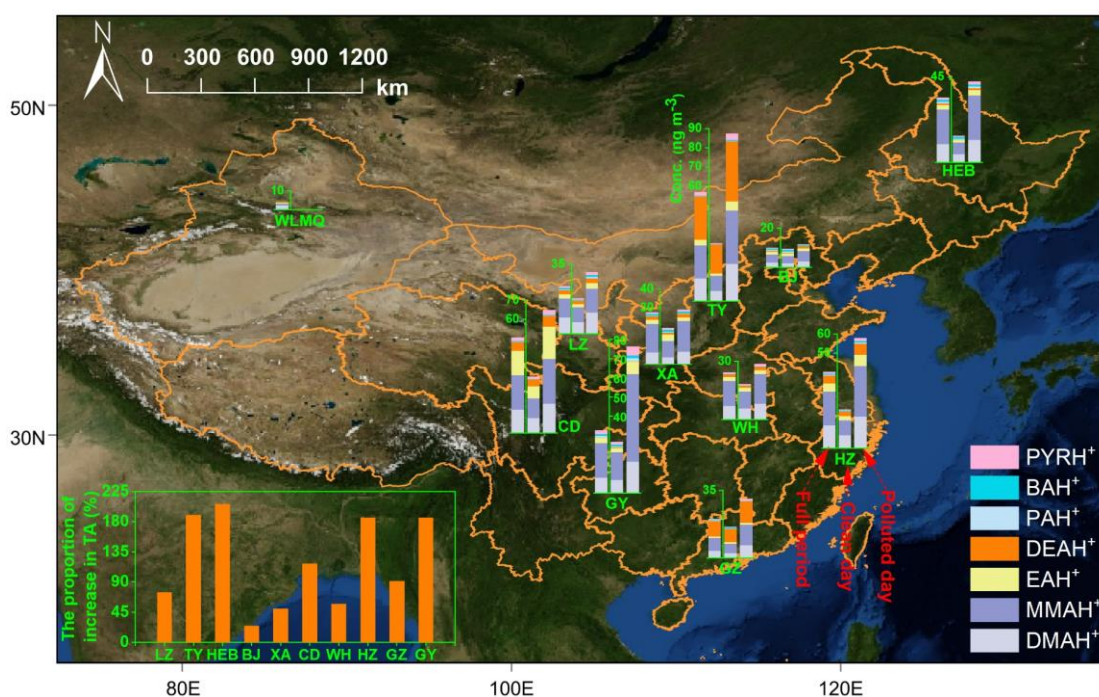
232 DEAH<sup>+</sup>) in PM<sub>2.5</sub> in all cities were not replaced by other aminiums from the clean  
233 days to the polluted days. This likely suggests that the main sources of atmospheric  
234 gas-phase amines in the cities did not change significantly on the polluted days. In  
235 addition, the proportions of MMAH<sup>+</sup> (solubility of 23.76 mol kg<sup>-1</sup> for aminium  
236 chloride form (Ge et al., 2011b)) and DMAH<sup>+</sup> (solubility of 44.80 mol kg<sup>-1</sup> for  
237 aminium chloride form (Ge et al., 2011b)) tended to further increase from the clean  
238 days to the polluted days, while that of DEAH<sup>+</sup> with relatively low solubility  
239 (solubility of 20.52 mol kg<sup>-1</sup> for aminium chloride form (Ge et al., 2011b)) showed a  
240 decreasing trend, especially in TY and GZ (where DEAH<sup>+</sup> was dominant). The  
241 concentrations of ALW in PM<sub>2.5</sub> were generally much higher on polluted days than on  
242 clean days, especially in the northern cities (**Tables S1–S3**). Clearly, liquid-phase  
243 processes likely played an important role in the formation of aminiums on polluted  
244 days.

245

### 246 **3.2. Aminium concentrations and their linkage with PM<sub>2.5</sub> variations**

247 **Figure 2** shows the average concentration distributions of various aminiums in  
248 PM<sub>2.5</sub> collected in different cities in China during winter, focusing on the difference  
249 between their concentrations on clean days and polluted days. The concentrations of  
250 total aminiums (TA) in TY ranged from 17.50 to 149.00 ng m<sup>-3</sup>, with an average of  
251  $56.90 \pm 41.81$  ng m<sup>-3</sup>. This average TA level was the highest among all the cities  
252 investigated. The average concentration of TA in WLMQ was found to be the lowest  
253 ( $4.16 \pm 1.24$  ng m<sup>-3</sup>), with a range of 2.10–6.50 ng m<sup>-3</sup>. As previously mentioned,

254 WLMQ is a vast city with a lower population density and less developed industries  
 255 compared to the more developed northern and coastal cities in China. Additionally,  
 256 this region is surrounded by barren mountains and sandy land (Ma et al., 2024)  
 257 (Figure 2). Apparently, the weak amine emission intensity appears to be responsible  
 258 for the low levels of aminiums in the WLMQ.



259  
 260 **Figure 2.** Average concentration distributions of various aminiums in PM<sub>2.5</sub> collected  
 261 in different cities in the winter in China. The stacked bar chart from left to right  
 262 indicates the data for the full sampling period, the clean day, and the polluted day in  
 263 turn. The column chart in the bottom left corner shows the proportion of the increase  
 264 in TA concentration from the clean days to the polluted days. The map was obtained  
 265 from ©MeteoInfoMap (version 3.3.0) (Chinese Academy of Meteorological Sciences,  
 266 China).

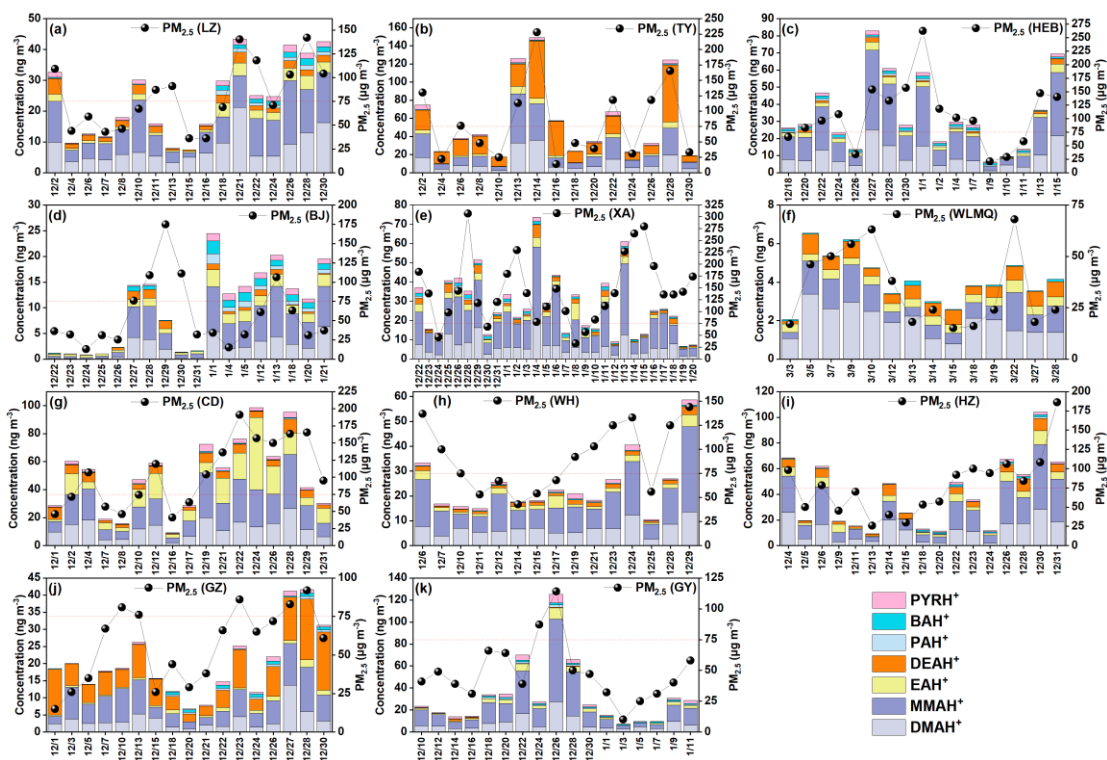
267

268 **Table S4** provides an overview of the aminiums detected in atmospheric fine

269 particles detected in different seasons and regions. The ranges of average TA  
270 concentrations in the northern cities (i.e., HEB, BJ, TY, XA, LZ, and WLMQ)  
271 generally overlapped with those measured in the coastal (GZ and HZ), central (WH),  
272 and southwestern (CD and GY) cities in this study (**Tables S1–S3**). Moreover, the  
273 average TA concentrations investigated here ( $4.16 \text{ ng m}^{-3} - 56.90 \text{ ng m}^{-3}$ ) were also  
274 within the observation ranges reported in previous studies ( $1.49 \text{ ng m}^{-3} - 329.80 \text{ ng m}^{-3}$ )  
275 **(Table S4)** (Ho et al., 2016; Liu et al., 2023; Shen et al., 2017; Huang et al., 2016;  
276 Choi et al., 2020; Liu et al., 2018; Shu et al., 2023). MMAH<sup>+</sup>, as the dominant  
277 aminium species in most of cities, showed the highest ( $18.33 \pm 12.82 \text{ ng m}^{-3}$ ) and  
278 lowest ( $1.07 \pm 0.55 \text{ ng m}^{-3}$ ) average concentrations in HEB and WLMQ, respectively.  
279 DEAH<sup>+</sup> was the most abundant aminium species in TY and GZ, with average  
280 concentrations of  $22.62 \pm 17.62 \text{ ng m}^{-3}$  and  $8.16 \pm 4.65 \text{ ng m}^{-3}$ , respectively (**Tables**  
281 **S1 and S3**). Two previous studies conducted in the GZ area in winter (2021 and 2015–  
282 2016) showed similar average DEAH<sup>+</sup> ( $\sim 7 \text{ ng m}^{-3}$ ) levels to this study (Liu et al.,  
283 2022b; Shu et al., 2023). However, DEAH<sup>+</sup> was not identified as the dominant  
284 aminium component in those two previous studies. Furthermore, lower aminium  
285 concentrations ( $< 8 \text{ ng m}^{-3}$ ) were generally found in most of the marine and polar  
286 regions (Dall’osto et al., 2019; Corral et al., 2022). In general, the concentration and  
287 composition of aminiums vary spatially, which may be attributed to spatial differences  
288 in amine sources, emission intensities, and the main factors affecting aminium  
289 formation.

290 The average concentrations of TA in all the investigated cities exhibited a similar

291 variation pattern from clean to polluted days, which was characterized by higher  
292 levels on polluted days (**Figure 2**). Specifically, the average aminium concentration  
293 showed an increase of up to 206% in HEB during the polluted period. TA  
294 concentrations in LZ, TY, CD, HZ, and GZ also increased greatly by 91% (in GZ)  
295 –190% (in TY). It seems that PM<sub>2.5</sub> pollution can be accompanied by an outbreak of  
296 aminiums. In contrast, a relatively small percentage increase in TA concentration  
297 during the polluted days was found in WH (57%), XA (50%), and BJ (25%). To  
298 further explore the linkage between changes in PM<sub>2.5</sub> and fluctuations in aminiums,  
299 the temporal variations in the mass concentrations of aminiums and PM<sub>2.5</sub> were  
300 compared across various cities (**Figure 3**). The concentrations of total and major  
301 aminiums in LZ, TY, HEB, WLMQ, CD, WH, HZ, GZ, and GY showed a temporal  
302 variation highly similar to that of PM<sub>2.5</sub>, as indicated by a significant correlation  
303 between TA and PM<sub>2.5</sub> in these cities ( $r = 0.61\text{--}0.85$ ,  $P < 0.05$ ). However, high levels  
304 of PM<sub>2.5</sub> can correspond to low levels of aminiums in XA (e.g., Dec. 29 and Jan. 2,  
305 14, 15, and 16) and BJ (e.g., Dec. 28, 30). The correlations between TA and PM<sub>2.5</sub> in  
306 these two cities were also insignificant ( $P > 0.05$ ). These results suggest that the  
307 formation of aminiums in XA and BJ during the polluted period may be constrained  
308 by some special factors, which will be discussed in the following discussion.



309

310 **Figure 3.** Temporal variations in the mass concentrations of aminiums and PM<sub>2.5</sub>  
 311 observed at the (a) LZ, (b) TY, (c) HEB, (d) BJ, (e) XA, (f) WLMQ, (g) CD, (h) WH,  
 312 (i) HZ, (j) GZ, and (k) GY sites.

313

### 314 3.3. Formation of aminiums and potential ammonia suppression in aminium 315 outbreaks

316 It is well documented that aminiums in PM<sub>2.5</sub> can be formed mainly via the  
 317 uptake of their gaseous form (i.e., amines) by aqueous particles, followed by acid-  
 318 base neutralization reactions (Ge et al., 2011b; Xie et al., 2018; Sauerwein and Chan,  
 319 2017; Qiu and Zhang, 2013; Liu et al., 2023). Clearly, the formation of particle-phase  
 320 aminiums was closely associated with the origins of the corresponding gas-phase  
 321 amines (as precursors of aminiums). We found that TA and major aminiums (e.g.,  
 322 MMAH<sup>+</sup>, DMAH<sup>+</sup>, and DEAH<sup>+</sup>) showed a significant positive correlation ( $P < 0.05$ )



323 with either SO<sub>2</sub>, NO<sub>2</sub>, or K<sup>+</sup> (as indicators of fuel combustion and biomass burning  
324 (Tian et al., 2020; Liu et al., 2023; Kunwar and Kawamura, 2014)) in LZ, TY, HEB,  
325 BJ, WLMQ, CD, WH, HZ, GZ, and GY (**Figure 4** and **Figure S2**). Thus, although  
326 lacking sufficient indicators (e.g., biogenic source traces) to trace the source of  
327 amines, our results can at least indicate that fossil fuel combustion or biomass burning  
328 may be important contributors to atmospheric amines in most of the investigated cities  
329 during the winter. This consideration was also supported by previous studies about the  
330 potential source analysis of aerosol aminiums in Guangzhou, Xuzhou, and Wulumuqi  
331 during the winter (Yang et al., 2023b; Shu et al., 2023; Ma et al., 2024). In contrast,  
332 the concentrations of TA in XA were weakly correlated ( $P > 0.05$ ) with those of K<sup>+</sup>,  
333 SO<sub>2</sub>, and NO<sub>2</sub>. Several studies conducted in XA have suggested that aerosol nitrogen-  
334 containing organic compounds can be largely derived from fossil fuel combustion and  
335 biomass burning (Zhang et al., 2023a; Zhang et al., 2023b; He et al., 2023; Yang et al.,  
336 2024). Moreover, the traditional method of identifying amine sources through  
337 correlation analysis (Berta et al., 2023; Liu et al., 2022b; Liu et al., 2022a; Huang et  
338 al., 2022; Corral et al., 2022) can also have significant uncertainties, as implied by the  
339 following two cases. First, the uptake of amines by aerosol particles might be  
340 constrained by low ALW concentration, weak particle acidity, or high ammonia levels  
341 (Liu et al., 2022b; Chen et al., 2022a; Ge et al., 2011b; Sauerwein and Chan, 2017;  
342 Chan and Chan, 2013; Wang et al., 2010). Second, amines might be largely  
343 decomposed by atmospheric oxidants (e.g., hydroxyl radical and ozone) (Nielsen et  
344 al., 2012; Qiu and Zhang, 2013). Thus, the abovementioned weak correlations

345 between aminiums and indicators in XA cannot definitely indicate that the  
 346 contributions of fossil fuel combustion and biomass burning to amines in XA were  
 347 insignificant. Presumably, the prerequisite for amine source apportionment using the  
 348 correlation between aminiums and indicators is that the gas-phase amines can be  
 349 largely converted into aminiums in PM<sub>2.5</sub> through secondary processes without the  
 350 influence of constrained factors. To further explore this issue, the following discussion  
 351 focuses on the main factors affecting the formation of aminiums in particles.



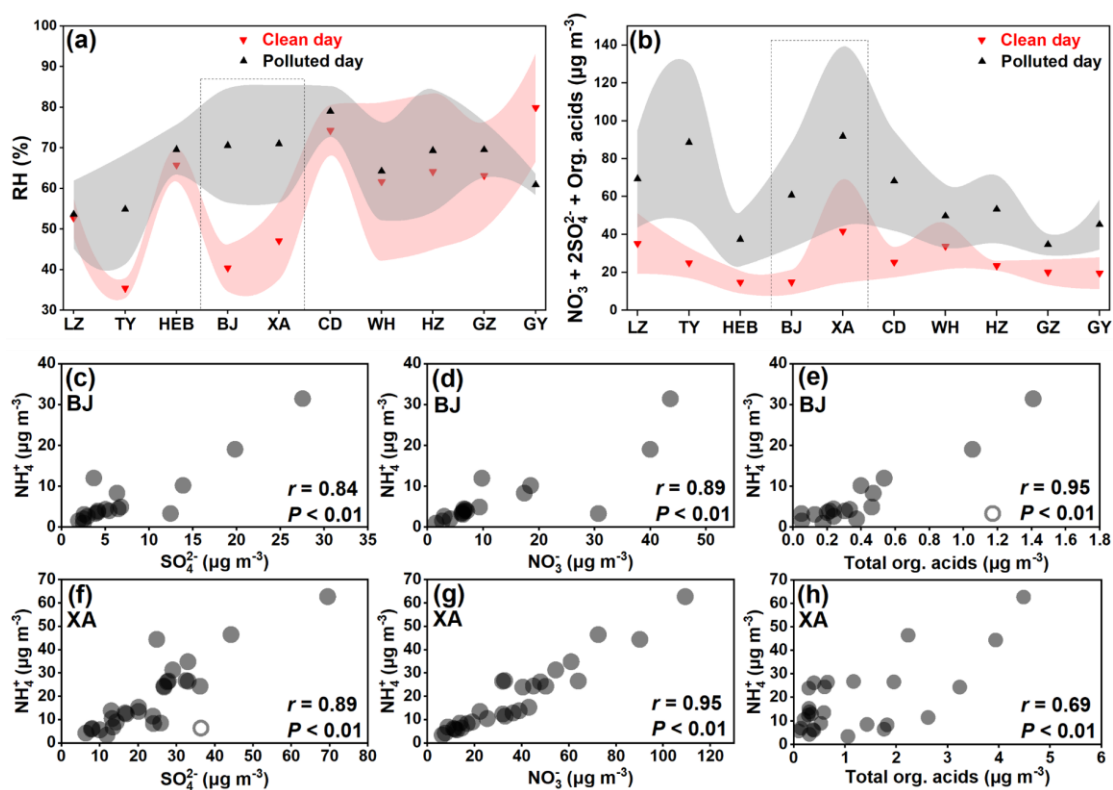
353 **Figure 4.** Diagrams presenting correlations between the concentrations of TA and  
 354 other parameters at (a–c) different sites. The colors of the different solid circles  
 355 indicate different correlation coefficients *r*. The size of the solid circle indicates the  
 356 significance of the correlation between the two corresponding parameters: the larger  
 357 circle indicates that the correlation is more significant, while the symbol “×” indicates  
 358 that the *P*-value is greater than 0.05.

359

360 The concentrations of TA in LZ, TY, HEB, WLMQ, CD, WH, HZ, GZ, and GY  
 361 showed significant positive correlations ( $P < 0.01$ ) with those of the acidic  
 362 components (e.g., NO<sub>3</sub><sup>-</sup>, SO<sub>4</sub><sup>2-</sup>, organic acids, and acidity (expressed as [(NO<sub>3</sub><sup>-</sup> +  
 363 2SO<sub>4</sub><sup>2-</sup>) – NH<sub>4</sub><sup>+</sup>] (Feng et al., 2022)), whereas an insignificant correlation ( $P > 0.05$ )  
 364 was found between them in BJ and XA (**Figure 4** and **Figure S3**). Thus, acid-base

365 chemistry was tightly associated with the formation of aminiums in PM<sub>2.5</sub> at all sites  
366 excepting BJ and XA. A recent laboratory study has suggested that amines can be  
367 neutralized by H<sub>3</sub>O<sup>+</sup> to form aminiums within picoseconds under conditions of high  
368 concentrations of particle sulfuric acid (Zhang et al., 2021). In addition, it has also  
369 been found that organic acids (e.g., formic acid) are able to participate in the  
370 nucleation of methanesulfonic acid–methylamine through an acid-base reaction  
371 (Zhang et al., 2022). The particles are acidic (especially on polluted days) at all study  
372 sites, with an average pH value ranging from 2.4 to 5.7 (**Tables S1–S3**). Amines can  
373 also partition into the particles by direct dissolution under high RH conditions (Ge et  
374 al., 2011b). Significantly increased RH values (i.e., high ALW) (**Figure 5a**) and acidic  
375 components (**Figure 5b**) on polluted days were also observed in XA and BJ.  
376 Nevertheless, the insignificant correlation between aminiums and acidic components  
377 and ALW concentrations in XA and BJ, together with a relatively small proportional  
378 increase in aminiums (**Figure 2**) from clean to polluted days at these two sites suggest  
379 that besides acidity and RH, there were other key factors affecting aminium formation  
380 in XA and BJ. As we know, the oxidative degradation of amines is one of the main  
381 pathways for the removal of atmospheric amines (Qiu and Zhang, 2013; Murphy et  
382 al., 2007). Furthermore, for atmospheric oxidants (e.g., hydroxyl radical) reacting  
383 with low-molecular-weight alkylamines, a negative temperature dependence of the  
384 rate coefficients has been reported (Nielsen et al., 2012). However, the winter air  
385 temperature in northern China was relatively low (< 0 °C in XA and BJ) (**Tables S1–**  
386 **S3**); moreover, there was no significant change in the atmospheric oxidation

387 (indicated by  $O_x$  levels ( $O_x = O_3 + NO_2$ )) of polluted and clean days in XA (higher  $O_x$   
 388 level during clean days) and BJ. In particular, the protonated amino group has been  
 389 suggested to be difficult to undergo oxidation by hydroxyl radicals and ozone  
 390 (Nielsen et al., 2012). Accordingly, atmospheric oxidation and temperature may not  
 391 be the main factors affecting changes in aminium concentrations from clean to  
 392 polluted days. Furthermore, the insignificant correlation between aminiums and acidic  
 393 components in XA and BJ suggests that other factors affecting aminium formation  
 394 must be considered.



395  
 396 **Figure 5.** The values of (a) RH and the concentrations of (b) major acidic  
 397 components (expressed as  $NO_3^- + 2SO_4^{2-} + \text{total organic acids}$ ) on clean and polluted  
 398 days in different cities. The triangle and the shaded area represent the mean value and  
 399 the associated standard deviation, respectively. The correlations of  $NH_4^+$  with the

400 concentrations of  $\text{NO}_3^-$ ,  $\text{SO}_4^{2-}$ , and total organic acids at (c–e) BJ and (f–h) XA. Open  
401 circles represent outliers.

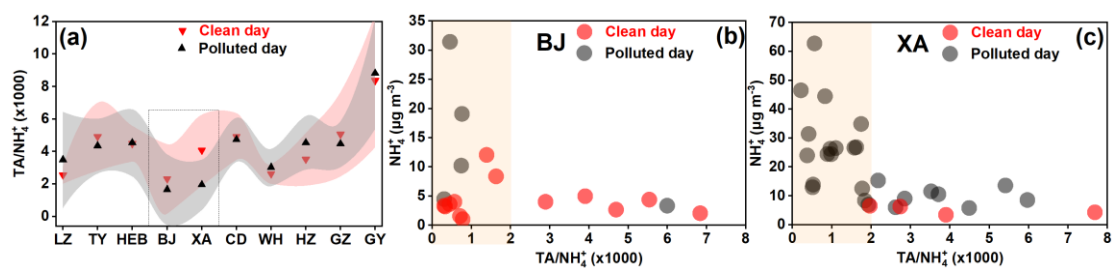
402

403 Furthermore, we found that the concentrations of  $\text{NH}_4^+$  were strongly ( $P < 0.01$ )  
404 correlated with those of acidic components in XA and BJ (**Figures 5c–h**). This  
405 indicates that the acidity of the particles was sufficient for the uptake of ammonia to  
406 form ammonium at these two study sites. Typically, the concentration of ammonia in  
407 the atmosphere is 1 to 3 orders of magnitude higher than that of low-molecular-weight  
408 alkylamines (Zheng et al., 2015; You et al., 2014; Yao et al., 2016; Wang et al., 2010).  
409 The uptake coefficient of alkylamines on acidic particles is lower than that of  
410 ammonia (Wang et al., 2010); moreover, Wang et al. (2010) proposed that fresh  
411  $\text{H}_2\text{SO}_4$  particles can be overwhelmingly neutralized by ammonia when both amines  
412 and ammonia are present in the air. In particular, although the strong acidic condition  
413 was conducive to the formation of aminiums, amines and ammonia may compete for  
414 uptake into acidic aerosol particles (Chen et al., 2022a). Thus, the constraint of  
415 ammonia on amine uptake at much higher ammonia levels than amine levels may be a  
416 possible explanation for the insignificant acid-dependent aminium formation in XA  
417 and BJ (**Figures 4a,b**).

418 To further explore the role of ammonia (or ammonium) in aminium formation,  
419 the average ratios of TA to  $\text{NH}_4^+$  on clean and polluted days in different cities were  
420 examined (**Figure 6a** and **Table S1–S3**). The average ratios of TA to  $\text{NH}_4^+$  were found  
421 to be lower in XA and BJ, especially on the polluted days, which was similar to the

422 characteristics of the TA/(NH<sub>3</sub> + NH<sub>4</sub><sup>+</sup>) ratios (**Figure S4**). The sensitivity analysis of  
423 the TA/NH<sub>4</sub><sup>+</sup> ratio (the lowest in XA and BJ) to NH<sub>4</sub><sup>+</sup> changes (**Figures 6b,c** and  
424 **Figure S5**) suggests that when TA/NH<sub>4</sub><sup>+</sup> > 2, the NH<sub>4</sub><sup>+</sup> concentrations in XA and BJ  
425 remained at a relatively low level (less than 6 μg m<sup>-3</sup> and 15 μg m<sup>-3</sup> in BJ and XA,  
426 respectively) with the increase of TA/NH<sub>4</sub><sup>+</sup> ratio, indicating that the formation of  
427 aminiums was not limited by ammonia at low amine and ammonium levels (in this  
428 case, TA was significantly ( $P < 0.01$ ) correlated with NH<sub>4</sub><sup>+</sup>). When TA/NH<sub>4</sub><sup>+</sup> < 2, the  
429 formation of aminiums may be constrained by higher amine and ammonium levels,  
430 which can also be supported by the insignificant ( $P > 0.05$ ) correlation between TA  
431 and NH<sub>4</sub><sup>+</sup> in this case. In contrast, the distributions of the ratios of TA to NH<sub>4</sub><sup>+</sup> in other  
432 cities were mainly in regions greater than 2 (**Figure S5**). The TA concentrations were  
433 thus significantly positively correlated with ammonium in these cities (excepting BJ  
434 and XA) (**Figure 4**). A recent study on the uptake of marine aerosol DMA by acidic  
435 aerosols has found that the concentrations of particle DMAH<sup>+</sup> generally decreased  
436 with increasing atmospheric ammonia concentrations (Chen et al., 2022a); moreover,  
437 these researchers proposed the possibility that aminiums can be displaced by  
438 ammonia in a high ammonia environment. Accordingly, high atmospheric ammonia  
439 levels can indeed constrain the conversion of amines to aminiums, even if the aerosol  
440 is acidic. In addition, due to the lower VC values (**Tables S1–S3**) on polluted days  
441 compared to clean days, the atmospheric amines were less able to diffuse on polluted  
442 days. This may result in an accumulation of aminiums on polluted days via acid-base  
443 chemistry. However, a large decrease in average TA/NH<sub>4</sub><sup>+</sup> and TA/(NH<sub>3</sub> + NH<sub>4</sub><sup>+</sup>) ratios

444 from clean to polluted days occurred in XA ( $t$ -Test,  $P < 0.05$ ) (Figure 6a, Figure S4,  
 445 and Table S1–S3), followed by BJ. These results indicate that the uptake of amines on  
 446 acidic particles relative to that of ammonia was significantly reduced from clean to  
 447 polluted days in XA. It should be noted that this reduced case may also occur in BJ,  
 448 while it is statistically insignificant. Presumably, the aminiums/ammonium ratio was  
 449 likely an important indicator to reveal the competitive uptake of ammonia against  
 450 amines on acidic aerosols, or the displacement of aminiums by ammonia in a high  
 451 ammonia environment. Thus, this study provides a special field case that emphasizes  
 452 the potential suppression of ammonia on aminium outbreaks during the polluted days.



453  
 454 **Figure 6.** The (a) average ratio of TA to NH<sub>4</sub><sup>+</sup> on clean and polluted days in different  
 455 cities. The triangle and the shaded area represent the mean value and the associated  
 456 standard deviation, respectively. Scatterplots of the mass concentration of NH<sub>4</sub><sup>+</sup> with  
 457 the ratio of TA to NH<sub>4</sub><sup>+</sup> at the (b) BJ and (c) XA sites.

#### 459 4. Conclusions and atmospheric implications

460 The concentrations, compositions, and temporal and spatial variations of  
 461 aminiums in PM<sub>2.5</sub> in 11 different Chinese cities during the winter were systematically  
 462 investigated to reveal the key factors affecting the aminium outbreak during the  
 463 polluted days. Specifically, MMAH<sup>+</sup> was the dominant species among the aminiums

464 investigated in  $PM_{2.5}$  in most cities, including LZ, XA, HEB, BJ, WLMQ, HZ, WH,  
465 CD, and GY, followed by  $DMAH^+$ . In contrast,  $DEAH^+$  was found to be the most  
466 abundant aminium species in TY and GZ, followed by  $MMAH^+$  and  $DMAH^+$ . This  
467 result can be attributed to the fact that the main sources of amines in TY and GZ were  
468 significantly different from those in other cities. However, due to the lack of amine  
469 emission inventories and sufficient tracers in these investigated cities, this study did  
470 not provide a detailed analysis of the specific sources of amines in these investigated  
471 cities.

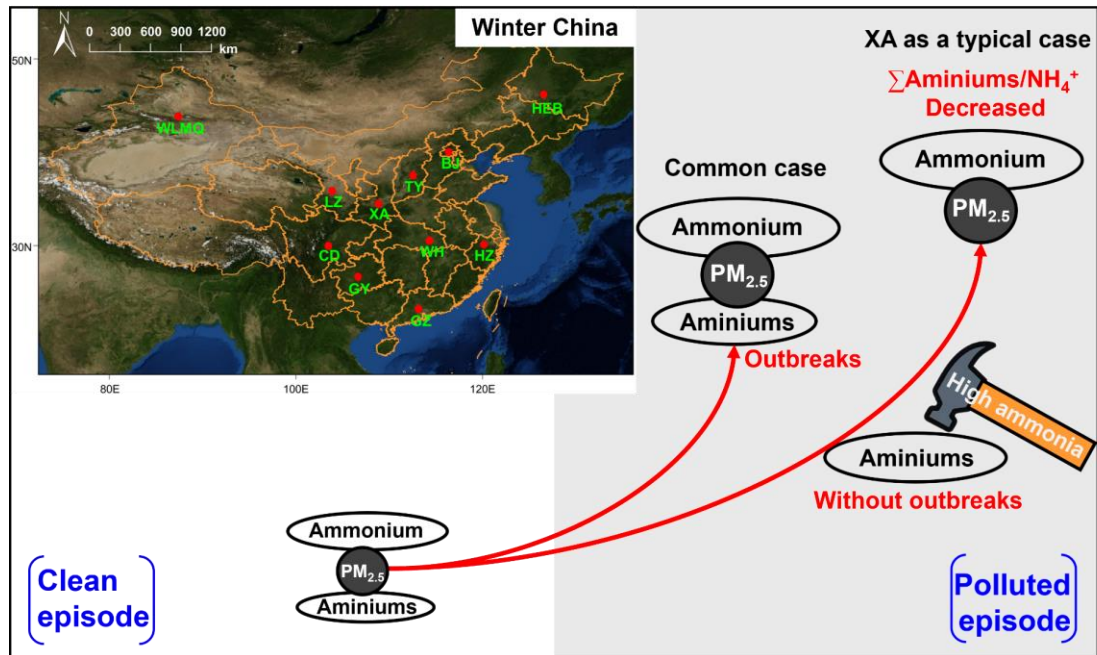
472 We found that the concentrations of TA and major aminiums in all cities showed  
473 a similar pattern of variation from the clean days to the polluted days, which was  
474 characterized by higher levels on the polluted days. However, the lowest percentage  
475 increase in TA concentration during the polluted days was found in XA (50%) and BJ  
476 (25%). Moreover, the concentrations of TA in XA and BJ were insignificantly ( $P >$   
477 0.05) correlated with those of  $PM_{2.5}$  and the main acidic components in  $PM_{2.5}$ .  
478 However, the significant correlations of TA with  $PM_{2.5}$  and the main acidic  
479 components were observed in other cities. Thus, acid-base chemistry was strongly  
480 associated with the formation of aminiums in  $PM_{2.5}$  in all cities with the exception of  
481 XA and BJ. The concentrations of  $NH_4^+$  were significantly ( $P < 0.01$ ) correlated with  
482 those of the acidic components in XA and BJ, indicating that the acidity of the  
483 particles was sufficient for the uptake of ammonia to form ammonium at these two  
484 sites. Further, based on the sensitivity analysis of the TA/ $NH_4^+$  ratio (the lowest in XA  
485 and BJ) to  $NH_4^+$  changes as well as excluding the effects of ALW and atmospheric



486 oxidation, we proposed a possibility about the competitive uptake of ammonia against  
487 amines on acidic aerosols in the ambient atmosphere in XA and BJ. This  
488 consideration may explain the insignificant acid-dependent aminium formation in XA  
489 and BJ. The main finding of this study has been illustrated in a diagram (**Figure 7**).

490 In general, this study has preliminarily explored the characteristics of aminiums,  
491 ammonium, and PM<sub>2.5</sub> from the clean days to the polluted days according to the  
492 observational data from 11 different Chinese cities, highlighting the possibility of the  
493 competitive uptake of ammonia versus amines on acidic aerosols, or the displacement  
494 of aminiums by ammonia under a high ammonia condition. Although a recent study  
495 has also demonstrated the possibility of individual aminium being displaced by  
496 ammonia in an environment of high ammonia level (Chen et al., 2022a), the uptake of  
497 amines on particles to form aminiums and **the mechanisms** of relevant influencing  
498 factors are still not fully understood. This is because acidity, environmental ammonia  
499 and amine content, temperature, and liquid-phase reactions all affect the uptake of  
500 amines, although acid-base neutralization of amines seems to be the most important  
501 pathway for amine uptake. Furthermore, if the uptake of amines is significantly  
502 constrained by the aforementioned factors, the traditional source apportionment  
503 methods using correlation analysis between particle aminiums and tracers will have  
504 significant uncertainty due to the weakened partitioning of the amines into the particle  
505 phase (i.e., causing insignificant correlations between aminiums and indicators).  
506 Further laboratory validation experiments are required to substantiate this inference.  
507 In addition, it is essential to conduct prolonged observational research in settings with

508 elevated ammonia levels and depleted amine concentrations in the near future.



509  
 510 **Figure 7.** Conceptual illustration showing the characteristics of aminiums,  
 511 ammonium, and PM<sub>2.5</sub> from the clean days to the polluted days. The map was  
 512 obtained from ©MeteoInfoMap (version 3.3.0) (Chinese Academy of Meteorological  
 513 Sciences, China).

514  
 515 **Data availability.** The data in this study are available at  
 516 <https://doi.org/10.5281/zenodo.11102019> (Xu et al., 2024).

517  
 518 **Supplement.** Four tables (Tables S1–S4) and five extensive figures (Figures S1–S5)  
 519 are provided in the Supplement. The supplement related to this article is available  
 520 online.

521

522 **Author contributions.** YX and HYX designed the study. YX, YJM, QBS, HWX, and  
523 HX performed field measurements and sample collection; TL performed chemical  
524 analysis; YX performed data analysis; YX wrote the original manuscript; and YX,  
525 HYX, and CQL reviewed and edited the manuscript.

526

527 **Competing interests.** The contact author has declared that none of the authors has  
528 any competing interests.

529

530 **Acknowledgements.** The authors are very grateful to the editor and the anonymous  
531 referees for the kind and valuable comments that improved the paper.

532

533 **Financial support.** This study has been kindly supported by the National Natural  
534 Science Foundation of China (grant no. 42303081) (Yu Xu) and the Shanghai Sailing  
535 Program of Shanghai Science and Technology Commission (grant no. 22YF1418700)  
536 (Yu Xu).

537

538 **Review statement.** This paper was edited by Roya Bahreini and reviewed by three  
539 anonymous referees.

540

## 541 **References**

542 Berta, V. Z., Russell, L. M., Price, D. J., Chen, C. L., Lee, A. K. Y., Quinn, P. K.,  
543 Bates, T. S., Bell, T. G., and Behrenfeld, M. J.: Non-volatile marine and non-

544 refractory continental sources of particle-phase amine during the North Atlantic  
545 Aerosols and Marine Ecosystems Study (NAAMES), *Atmos. Chem. Phys.*, 23, 2765-  
546 2787, 10.5194/acp-23-2765-2023, 2023.

547 Chan, L. P. and Chan, C. K.: Role of the Aerosol Phase State in  
548 Ammonia/Amines Exchange Reactions, *Environmental Science & Technology*, 47,  
549 5755-5762, 10.1021/es4004685, 2013.

550 Chang, Y., Wang, H., Gao, Y., Jing, S. a., Lu, Y., Lou, S., Kuang, Y., Cheng, K.,  
551 Ling, Q., Zhu, L., Tan, W., and Huang, R.-J.: Nonagricultural Emissions Dominate  
552 Urban Atmospheric Amines as Revealed by Mobile Measurements, *Geophysical*  
553 *Research Letters*, 49, e2021GL097640, <https://doi.org/10.1029/2021GL097640>, 2022.

554 Chen, D., Yao, X., Chan, C. K., Tian, X., Chu, Y., Clegg, S. L., Shen, Y., Gao, Y.,  
555 and Gao, H.: Competitive Uptake of Dimethylamine and Trimethylamine against  
556 Ammonia on Acidic Particles in Marine Atmospheres, *Environmental Science &*  
557 *Technology*, 56, 5430-5439, 10.1021/acs.est.1c08713, 2022a.

558 Chen, Y., Lin, Q., Li, G., and An, T.: A new method of simultaneous  
559 determination of atmospheric amines in gaseous and particulate phases by gas  
560 chromatography-mass spectrometry, *Journal of Environmental Sciences*, 114, 401-  
561 411, <https://doi.org/10.1016/j.jes.2021.09.027>, 2022b.

562 Chen, Y., Tian, M., Huang, R. J., Shi, G., Wang, H., Peng, C., Cao, J., Wang, Q.,  
563 Zhang, S., Guo, D., Zhang, L., and Yang, F.: Characterization of urban amine-  
564 containing particles in southwestern China: seasonal variation, source, and processing,  
565 *Atmos. Chem. Phys.*, 19, 3245-3255, 10.5194/acp-19-3245-2019, 2019.

566 Choi, N. R., Lee, J. Y., Ahn, Y. G., and Kim, Y. P.: Determination of atmospheric  
567 amines at Seoul, South Korea via gas chromatography/tandem mass spectrometry,  
568 *Chemosphere*, 258, 127367, 10.1016/j.chemosphere.2020.127367, 2020.

569 Corral, A. F., Choi, Y., Collister, B. L., Crosbie, E., Dadashazar, H., DiGangi, J.  
570 P., Diskin, G. S., Fenn, M., Kirschler, S., Moore, R. H., Nowak, J. B., Shook, M. A.,  
571 Stahl, C. T., Shingler, T., Thornhill, K. L., Voigt, C., Ziemba, L. D., and Sorooshian,  
572 A.: Dimethylamine in cloud water: a case study over the northwest Atlantic Ocean,  
573 *Environmental Science: Atmospheres*, 2, 1534-1550, 10.1039/D2EA00117A, 2022.

574 Dall'Osto, M., Airs, R. L., Beale, R., Cree, C., Fitzsimons, M. F., Beddows, D.,  
575 Harrison, R. M., Ceburnis, D., O'Dowd, C., Rinaldi, M., Paglione, M., Nenes, A.,  
576 Decesari, S., and Simó, R.: Simultaneous Detection of Alkylamines in the Surface  
577 Ocean and Atmosphere of the Antarctic Sympagic Environment, *ACS Earth and*  
578 *Space Chemistry*, 3, 854-862, 10.1021/acsearthspacechem.9b00028, 2019.

579 Facchini, M. C., Decesari, S., Rinaldi, M., Carbone, C., Finessi, E., Mircea, M.,  
580 Fuzzi, S., Moretti, F., Tagliavini, E., Ceburnis, D., and O'Dowd, C. D.: Important  
581 Source of Marine Secondary Organic Aerosol from Biogenic Amines, *Environmental*  
582 *Science & Technology*, 42, 9116-9121, 10.1021/es8018385, 2008.

583 Feng, X., Wang, C., Feng, Y., Cai, J., Zhang, Y., Qi, X., Li, Q., Li, J., and Chen,  
584 Y.: Outbreaks of Ethyl-Amines during Haze Episodes in North China Plain: A  
585 Potential Source of Amines from Ethanol Gasoline Vehicle Emission, *Environmental*  
586 *Science & Technology Letters*, 9, 306-311, 10.1021/acs.estlett.2c00145, 2022.

587 Gani, S., Bhandari, S., Seraj, S., Wang, D. S., Patel, K., Soni, P., Arub, Z., Habib,

588 G., Hildebrandt Ruiz, L., and Apte, J. S.: Submicron aerosol composition in the  
589 world's most polluted megacity: the Delhi Aerosol Supersite study, *Atmos. Chem.*  
590 *Phys.*, 19, 6843-6859, 10.5194/acp-19-6843-2019, 2019.

591 Ge, X., Wexler, A. S., and Clegg, S. L.: Atmospheric amines – Part I. A review,  
592 *Atmospheric Environment*, 45, 524-546,  
593 <https://doi.org/10.1016/j.atmosenv.2010.10.012>, 2011a.

594 Ge, X., Wexler, A. S., and Clegg, S. L.: Atmospheric amines – Part II.  
595 Thermodynamic properties and gas/particle partitioning, *Atmospheric Environment*,  
596 45, 561-577, <https://doi.org/10.1016/j.atmosenv.2010.10.013>, 2011b.

597 Gibb, S. W., Mantoura, R. F. C., and Liss, P. S.: Ocean-atmosphere exchange and  
598 atmospheric speciation of ammonia and methylamines in the region of the NW  
599 Arabian Sea, *Global Biogeochemical Cycles*, 13, 161-178,  
600 <https://doi.org/10.1029/98GB00743>, 1999.

601 He, K., Fu, T., Zhang, B., Xu, H., Sun, J., Zou, H., Zhang, Z., Hang Ho, S. S.,  
602 Cao, J., and Shen, Z.: Examination of long-time aging process on volatile organic  
603 compounds emitted from solid fuel combustion in a rural area of China,  
604 *Chemosphere*, 333, 138957, <https://doi.org/10.1016/j.chemosphere.2023.138957>,  
605 2023.

606 Ho, K.-F., Ho, S. S. H., Huang, R.-J., Chuang, H.-C., Cao, J.-J., Han, Y., Lui, K.-  
607 H., Ning, Z., Chuang, K.-J., Cheng, T.-J., Lee, S.-C., Hu, D., Wang, B., and Zhang,  
608 R.: Chemical composition and bioreactivity of PM<sub>2.5</sub> during 2013 haze events in  
609 China, *Atmospheric Environment*, 126, 162-170,

610 <https://doi.org/10.1016/j.atmosenv.2015.11.055>, 2016.

611 Ho, K. F., Ho, S. S. H., Huang, R.-J., Liu, S. X., Cao, J.-J., Zhang, T., Chuang,  
612 H.-C., Chan, C. S., Hu, D., and Tian, L.: Characteristics of water-soluble organic  
613 nitrogen in fine particulate matter in the continental area of China, *Atmospheric*  
614 *Environment*, 106, 252-261, <https://doi.org/10.1016/j.atmosenv.2015.02.010>, 2015.

615 Huang, S., Song, Q., Hu, W., Yuan, B., Liu, J., Jiang, B., Li, W., Wu, C., Jiang,  
616 F., Chen, W., Wang, X., and Shao, M.: Chemical composition and sources of amines  
617 in PM<sub>2.5</sub> in an urban site of PRD, China, *Environmental Research*, 212, 113261,  
618 <https://doi.org/10.1016/j.envres.2022.113261>, 2022.

619 Huang, X., Deng, C., Zhuang, G., Lin, J., and Xiao, M.: Quantitative analysis of  
620 aliphatic amines in urban aerosols based on online derivatization and high  
621 performance liquid chromatography, *Environmental Science: Processes & Impacts*,  
622 18, 796-801, 10.1039/C6EM00197A, 2016.

623 Kunwar, B. and Kawamura, K.: One-year observations of carbonaceous and  
624 nitrogenous components and major ions in the aerosols from subtropical Okinawa  
625 Island, an outflow region of Asian dusts, *Atmos. Chem. Phys.*, 14, 1819-1836.  
626 <https://doi.org/10.5194/acp-14-1819-2014>, 2014.

627 Li, G., Liao, Y., Hu, J., Lu, L., Zhang, Y., Li, B., and An, T.: Activation of NF- $\kappa$ B  
628 pathways mediating the inflammation and pulmonary diseases associated with  
629 atmospheric methylamine exposure, *Environmental pollution*, 252, 1216-1224,  
630 <https://doi.org/10.1016/j.envpol.2019.06.059>, 2019.

631 Lin, X., Xu, Y., Zhu, R.-G., Xiao, H.-W., and Xiao, H.-Y.: Proteinaceous Matter

632 in PM<sub>2.5</sub> in Suburban Guiyang, Southwestern China: Decreased Importance in Long-  
633 Range Transport and Atmospheric Degradation, *J. Geophys. Res.: Atmos.*, 128,  
634 e2023JD038516, <https://doi.org/10.1029/2023JD038516>, 2023.

635 Liu, C., Li, H., Zheng, H., Wang, G., Qin, X., Chen, J., Zhou, S., Lu, D., Liang,  
636 G., Song, X., Duan, Y., Liu, J., Huang, K., and Deng, C.: Ocean Emission Pathway  
637 and Secondary Formation Mechanism of Aminiums Over the Chinese Marginal Sea,  
638 *Journal of Geophysical Research: Atmospheres*, 127, e2022JD037805,  
639 <https://doi.org/10.1029/2022JD037805>, 2022a.

640 Liu, F., Bi, X., Zhang, G., Peng, L., Lian, X., Lu, H., Fu, Y., Wang, X., Peng, P.  
641 a., and Sheng, G.: Concentration, size distribution and dry deposition of amines in  
642 atmospheric particles of urban Guangzhou, China, *Atmospheric Environment*, 171,  
643 279-288, <https://doi.org/10.1016/j.atmosenv.2017.10.016>, 2017.

644 Liu, F., Zhang, G., Lian, X., Fu, Y., Lin, Q., Yang, Y., Bi, X., Wang, X., Peng, P.  
645 a., and Sheng, G.: Influence of meteorological parameters and oxidizing capacity on  
646 characteristics of airborne particulate amines in an urban area of the Pearl River Delta,  
647 *China, Environmental Research*, 212, 113212,  
648 <https://doi.org/10.1016/j.envres.2022.113212>, 2022b.

649 Liu, F., Bi, X., Zhang, G., Lian, X., Fu, Y., Yang, Y., Lin, Q., Jiang, F., Wang, X.,  
650 Peng, P. a., and Sheng, G.: Gas-to-particle partitioning of atmospheric amines  
651 observed at a mountain site in southern China, *Atmospheric Environment*, 195, 1-11,  
652 <https://doi.org/10.1016/j.atmosenv.2018.09.038>, 2018.

653 Liu, T., Xu, Y., Sun, Q.-B., Xiao, H.-W., Zhu, R.-G., Li, C.-X., Li, Z.-Y., Zhang,



654 K.-Q., Sun, C.-X., and Xiao, H.-Y.: Characteristics, Origins, and Atmospheric  
655 Processes of Amines in Fine Aerosol Particles in Winter in China, *J. Geophys. Res.:*  
656 *Atmos.*, 128, e2023JD038974, <https://doi.org/10.1029/2023JD038974>, 2023.

657 Liu, Z., Li, M., Wang, X., Liang, Y., Jiang, Y., Chen, J., Mu, J., Zhu, Y., Meng,  
658 H., Yang, L., Hou, K., Wang, Y., and Xue, L.: Large contributions of anthropogenic  
659 sources to amines in fine particles at a coastal area in northern China in winter,  
660 *Science of The Total Environment*, 839, 156281,  
661 <https://doi.org/10.1016/j.scitotenv.2022.156281>, 2022c.

662 Ma, Y. J., Xu, Y., Yang, T., Xiao, H. W., and Xiao, H. Y.: Measurement report:  
663 Characteristics of nitrogen-containing organics in PM<sub>2.5</sub> in Ürümqi, northwestern  
664 China – differential impacts of combustion of fresh and aged biomass materials,  
665 *Atmos. Chem. Phys.*, 24, 4331-4346, 10.5194/acp-24-4331-2024, 2024.

666 Møller, K. H., Berndt, T., and Kjaergaard, H. G.: Atmospheric Autoxidation of  
667 Amines, *Environmental Science & Technology*, 54, 11087-11099,  
668 10.1021/acs.est.0c03937, 2020.

669 Murphy, S. M., Sorooshian, A., Kroll, J. H., Ng, N. L., Chhabra, P., Tong, C.,  
670 Surratt, J. D., Knipping, E., Flagan, R. C., and Seinfeld, J. H.: Secondary aerosol  
671 formation from atmospheric reactions of aliphatic amines, *Atmos. Chem. Phys.*, 7,  
672 2313-2337, 10.5194/acp-7-2313-2007, 2007.

673 Nielsen, C. J., Herrmann, H., and Weller, C.: Atmospheric chemistry and  
674 environmental impact of the use of amines in carbon capture and storage (CCS),  
675 *Chemical Society Reviews*, 41, 6684-6704, 10.1039/C2CS35059A, 2012.

676 Qiu, C. and Zhang, R.: Multiphase chemistry of atmospheric amines, *Physical*  
677 *Chemistry Chemical Physics*, 15, 5738-5752, 10.1039/C3CP43446J, 2013.

678 Sauerwein, M. and Chan, C. K.: Heterogeneous uptake of ammonia and  
679 dimethylamine into sulfuric and oxalic acid particles, *Atmos. Chem. Phys.*, 17, 6323-  
680 6339, 10.5194/acp-17-6323-2017, 2017.

681 Shen, W., Ren, L., Zhao, Y., Zhou, L., Dai, L., Ge, X., Kong, S., Yan, Q., Xu, H.,  
682 Jiang, Y., He, J., Chen, M., and Yu, H.: C1-C2 alkyl aminiums in urban aerosols:  
683 Insights from ambient and fuel combustion emission measurements in the Yangtze  
684 River Delta region of China, *Environmental pollution*, 230, 12-21,  
685 <https://doi.org/10.1016/j.envpol.2017.06.034>, 2017.

686 Shen, X., Chen, J., Li, G., and An, T.: A new advance in the pollution profile,  
687 transformation process, and contribution to aerosol formation and aging of  
688 atmospheric amines, *Environmental Science: Atmospheres*, 3, 444-473,  
689 10.1039/D2EA00167E, 2023.

690 Shu, Q., Pei, C., Lin, X., Hong, D., Lai, S., and Zhang, Y.: Variations of  
691 aminiums in fine particles at a suburban site in Guangzhou, China: Importance of  
692 anthropogenic and natural emissions, *Particuology*, 80, 140-147,  
693 <https://doi.org/10.1016/j.partic.2022.11.019>, 2023.

694 Tao, Y., Liu, T., Yang, X., and Murphy, J. G.: Kinetics and Products of the  
695 Aqueous Phase Oxidation of Triethylamine by OH, *ACS Earth and Space Chemistry*,  
696 5, 1889-1895, 10.1021/acsearthspacechem.1c00162, 2021.

697 Tao, Y., Ye, X., Jiang, S., Yang, X., Chen, J., Xie, Y., and Wang, R.: Effects of

698 amines on particle growth observed in new particle formation events, *Journal of*  
699 *Geophysical Research: Atmospheres*, 121, 324-335,  
700 <https://doi.org/10.1002/2015JD024245>, 2016.

701 Tian, D., Fan, J., Jin, H., Mao, H., Geng, D., Hou, S., Zhang, P., and Zhang, Y.:  
702 Characteristic and Spatiotemporal Variation of Air Pollution in Northern China Based  
703 on Correlation Analysis and Clustering Analysis of Five Air Pollutants, *Journal of*  
704 *Geophysical Research: Atmospheres*, 125, e2019JD031931,  
705 <https://doi.org/10.1029/2019JD031931>, 2020.

706 Tong, D., Chen, J., Qin, D., Ji, Y., Li, G., and An, T.: Mechanism of atmospheric  
707 organic amines reacted with ozone and implications for the formation of secondary  
708 organic aerosols, *Science of The Total Environment*, 737, 139830,  
709 <https://doi.org/10.1016/j.scitotenv.2020.139830>, 2020.

710 Wang, L., Lal, V., Khalizov, A. F., and Zhang, R.: Heterogeneous Chemistry of  
711 Alkylamines with Sulfuric Acid: Implications for Atmospheric Formation of  
712 Alkylammonium Sulfates, *Environmental Science & Technology*, 44, 2461-2465,  
713 [10.1021/es9036868](https://doi.org/10.1021/es9036868), 2010.

714 Wang, M., Wang, Q., Ho, S. S. H., Li, H., Zhang, R., Ran, W., Qu, L., Lee, S.-c.,  
715 and Cao, J.: Chemical characteristics and sources of nitrogen-containing organic  
716 compounds at a regional site in the North China Plain during the transition period of  
717 autumn and winter, *Science of The Total Environment*, 812, 151451,  
718 <https://doi.org/10.1016/j.scitotenv.2021.151451>, 2022.

719 Xie, H., Feng, L., Hu, Q., Zhu, Y., Gao, H., Gao, Y., and Yao, X.: Concentration

720 and size distribution of water-extracted dimethylammonium and trimethylammonium in  
721 atmospheric particles during nine campaigns - Implications for sources, phase states  
722 and formation pathways, *Science of The Total Environment*, 631-632, 130-141,  
723 <https://doi.org/10.1016/j.scitotenv.2018.02.303>, 2018.

724 Xu, Y., Dong, X.-N., Xiao, H.-Y., He, C., and Wu, D.-S.: Water-Insoluble  
725 Components in Rainwater in Suburban Guiyang, Southwestern China: A Potential  
726 Contributor to Dissolved Organic Carbon, *Journal of Geophysical Research:*  
727 *Atmospheres*, 127, e2022JD037721, <https://doi.org/10.1029/2022JD037721>, 2022a.

728 Xu, Y., Dong, X.-N., Xiao, H.-Y., Zhou, J.-X., and Wu, D.-S.: Proteinaceous  
729 Matter and Liquid Water in Fine Aerosols in Nanchang, Eastern China: Seasonal  
730 Variations, Sources, and Potential Connections, *J. Geophys. Res.: Atmos.*, 127,  
731 e2022JD036589. <https://doi.org/10.1029/2022JD036589>, 2022b.

732 Xu, Y., Dong, X. N., He, C., Wu, D. S., Xiao, H. W., and Xiao, H. Y.: Mist  
733 cannon trucks can exacerbate the formation of water-soluble organic aerosol and  
734 PM<sub>2.5</sub> pollution in the road environment, *Atmos. Chem. Phys.*, 23, 6775-6788,  
735 [10.5194/acp-23-6775-2023](https://doi.org/10.5194/acp-23-6775-2023), 2023.

736 Xu, Y., Miyazaki, Y., Tachibana, E., Sato, K., Ramasamy, S., Mochizuki, T.,  
737 Sadanaga, Y., Nakashima, Y., Sakamoto, Y., Matsuda, K., and Kajii, Y.: Aerosol  
738 Liquid Water Promotes the Formation of Water-Soluble Organic Nitrogen in  
739 Submicrometer Aerosols in a Suburban Forest, *Environ. Sci. Technol.*, 54, 1406-1414.  
740 <https://doi.org/10.1021/acs.est.1409b05849>, 2020.

741 Yang, T., Xu, Y., Ye, Q., Ma, Y. J., Wang, Y. C., Yu, J. Z., Duan, Y. S., Li, C. X.,

742 Xiao, H. W., Li, Z. Y., Zhao, Y., and Xiao, H. Y.: Spatial and diurnal variations of  
743 aerosol organosulfates in summertime Shanghai, China: potential influence of  
744 photochemical processes and anthropogenic sulfate pollution, *Atmos. Chem. Phys.*,  
745 23, 13433-13450, 10.5194/acp-23-13433-2023, 2023a.

746 Yang, X.-Y., Cao, F., Fan, M.-Y., Lin, Y.-C., Xie, F., and Zhang, Y.-L.: Seasonal  
747 variations of low molecular alkyl amines in PM<sub>2.5</sub> in a North China Plain industrial  
748 city: Importance of secondary formation and combustion emissions, *Science of The  
749 Total Environment*, 857, 159371, <https://doi.org/10.1016/j.scitotenv.2022.159371>,  
750 2023b.

751 Yang, X., Huang, S., Li, D., Xu, H., Zeng, Y., Yang, L., Wang, D., Zhang, N.,  
752 Cao, J., and Shen, Z.: Water-soluble organic matter with various polarities in PM<sub>2.5</sub>  
753 over Xi'an, China: Abundance, functional groups, and light absorption, *Particuology*,  
754 84, 281-289, <https://doi.org/10.1016/j.partic.2023.07.005>, 2024.

755 Yao, L., Wang, M. Y., Wang, X. K., Liu, Y. J., Chen, H. F., Zheng, J., Nie, W.,  
756 Ding, A. J., Geng, F. H., Wang, D. F., Chen, J. M., Worsnop, D. R., and Wang, L.:  
757 Detection of atmospheric gaseous amines and amides by a high-resolution time-of-  
758 flight chemical ionization mass spectrometer with protonated ethanol reagent ions,  
759 *Atmos. Chem. Phys.*, 16, 14527-14543, 10.5194/acp-16-14527-2016, 2016.

760 Yao, L., Garmash, O., Bianchi, F., Zheng, J., Yan, C., Kontkanen, J., Junninen,  
761 H., Mazon, S. B., Ehn, M., Paasonen, P., Sipilä, M., Wang, M., Wang, X., Xiao, S.,  
762 Chen, H., Lu, Y., Zhang, B., Wang, D., Fu, Q., Geng, F., Li, L., Wang, H., Qiao, L.,  
763 Yang, X., Chen, J., Kerminen, V.-M., Petäjä, T., Worsnop, D. R., Kulmala, M., and

764 Wang, L.: Atmospheric new particle formation from sulfuric acid and amines in a  
765 Chinese megacity, *Science*, 361, 278-281, doi:10.1126/science.aao4839, 2018.

766 You, Y., Kanawade, V. P., de Gouw, J. A., Guenther, A. B., Madronich, S., Sierra-  
767 Hernández, M. R., Lawler, M., Smith, J. N., Takahama, S., Ruggeri, G., Koss, A.,  
768 Olson, K., Baumann, K., Weber, R. J., Nenes, A., Guo, H., Edgerton, E. S., Porcelli,  
769 L., Brune, W. H., Goldstein, A. H., and Lee, S. H.: Atmospheric amines and ammonia  
770 measured with a chemical ionization mass spectrometer (CIMS), *Atmos. Chem.*  
771 *Phys.*, 14, 12181-12194, 10.5194/acp-14-12181-2014, 2014.

772 Zhang, B., Shen, Z., He, K., Sun, J., Huang, S., Xu, H., Li, J., Ho, S. S. H., and  
773 Cao, J.-j.: Insight into the Primary and Secondary Particle-Bound Methoxyphenols  
774 and Nitroaromatic Compound Emissions from Solid Fuel Combustion and the  
775 Updated Source Tracers, *Environmental Science & Technology*, 57, 14280-14288,  
776 10.1021/acs.est.3c04370, 2023a.

777 Zhang, B., Shen, Z., He, K., Zhang, L., Huang, S., Sun, J., Xu, H., Li, J., Yang,  
778 L., and Cao, J.: Source Profiles of Particle-Bound Phenolic Compounds and Aromatic  
779 Acids From Fresh and Aged Solid Fuel Combustion: Implication for the Aging  
780 Mechanism and Newly Proposed Source Tracers, *Journal of Geophysical Research:*  
781 *Atmospheres*, 128, e2023JD039758, <https://doi.org/10.1029/2023JD039758>, 2023b.

782 Zhang, R., Shen, J., Xie, H. B., Chen, J., and Elm, J.: The role of organic acids in  
783 new particle formation from methanesulfonic acid and methylamine, *Atmos. Chem.*  
784 *Phys.*, 22, 2639-2650, 10.5194/acp-22-2639-2022, 2022.

785 Zhang, W., Zhong, J., Shi, Q., Gao, L., Ji, Y., Li, G., An, T., and Francisco, J. S.:

786 Mechanism for Rapid Conversion of Amines to Ammonium Salts at the Air–Particle  
787 Interface, *Journal of the American Chemical Society*, 143, 1171-1178,  
788 10.1021/jacs.0c12207, 2021.

789 Zhang, Y.-L. and Cao, F.: Fine particulate matter (PM<sub>2.5</sub>) in China at a city level,  
790 *Scientific Reports*, 5, 14884, 10.1038/srep14884, 2015.

791 Zheng, J., Ma, Y., Chen, M., Zhang, Q., Wang, L., Khalizov, A. F., Yao, L.,  
792 Wang, Z., Wang, X., and Chen, L.: Measurement of atmospheric amines and ammonia  
793 using the high resolution time-of-flight chemical ionization mass spectrometry,  
794 *Atmospheric Environment*, 102, 249-259,  
795 <https://doi.org/10.1016/j.atmosenv.2014.12.002>, 2015.

796